First-order irreversible phase transitions in a nonequilibrium system: Mean-field analysis and simulation results

Roberto A. Monetti*
Instituto de Investigaciones Fisicoquímicas Teóricas y Aplicadas (INIFTA), UNLP, CONICET, CIC (Bs. As.), C. C. 16 Suc. 4, 1900 La Plata, Argentina

(Received 13 June 2001; published 5 December 2001)

First-order irreversible phase transitions (IPT's) between an active regime and an absorbing state are studied in a single-component, two-dimensional interacting particle system by means of both simulations and a mean-field analysis. Several features obtained using the mean-field approximation such as the presence of a first-order IPT and hysteresis effects, are in excellent agreement with simulation results. In addition, extensive epidemic simulations show that the dynamical critical behavior of the system is by no means scale invariant.

DOI: 10.1103/PhysRevE.65.016103 PACS number(s): 64.60.Ht, 05.70.Jk, 02.50.Ey, 82.65.+r

I. INTRODUCTION

The study of nonequilibrium systems is relevant to a broad scope of phenomena in diverse areas of research such as physics, chemistry, ecology, catalysis, economy, and social sciences, etc. [1–3]. An intriguing feature of some of these systems is the occurrence of irreversible phase transitions (IPT's) between an active regime and an absorbing state where the system becomes trapped. Typically, continuous transitions to a unique absorbing state belong to the directed percolation (DP) universality class [4,5]. DP critical behavior is observed over wide-ranging problems emerging from different disciplines such as quantum particle physics [6], irreversible catalytic systems [3,7,8], and contact processes [9]. Several models with infinitely many absorbing configurations have been proposed but no new universality class has been found [10]. Thus, the DP universality class is apparently extremely robust. In contrast to the above-mentioned phase transition to infinitely many absorbing configurations that belongs to the DP class, a new type of IPT's to multiple absorbing states has recently been considered. In these systems, the activity is coupled to a field conserved by the dynamics. Due to this coupling, a new universality class arises that seems to gather systems with infinitely many absorbing configurations where the order parameter is coupled to a conserved field [11].

There is another group of models whose critical behavior belong to a new universality class different from DP [12]. A relevant feature is shared by these models. The number of particles is conserved modulo 2. This is the reason why this class is often called parity conserving universality class. The great activity in the field of second-order continuous IPT's has led us to a good understanding of such a systems. Unfortunately, continuous IPT's have never been observed in experiments and consequently most of the activity in the field is mainly of theoretical interest.

On the other hand, it is discontinuous or first-order IPT's that are most commonly observed in experiments [13]. In spite of this fact, discontinuous IPT's have not received as much attention as continuous IPT's. Early results [14,15] claiming the existence of scale invariance in the dynamical critical behavior of first-order IPT's were based on inadequately short-time simulations. However, very recently, we have shown by means of extended simulations that the asymptotic dynamical critical behavior is exponentially decaying [16]. A similar controversy has also arisen in the field of reversible transitions [17]. In this case, the power-law behavior is identified as a finite-size effect that vanishes in the thermodynamic limit. Furthermore, the existence of hysteresis, which is a signature of first-order transitions in equilibrium systems, has so far, not been explored in detail in the field of IPT's.

The aim of this work is to present a detailed study of the first-order irreversible critical behavior observed in a two-dimensional (2D) cellular automaton, called the ''stochastic game of life'' (SGL) [15], based on two complementary techniques, namely, extensive numerical simulations and a mean-field approach. The SGL was inspired by the deterministic Conway's ''game of life'' [18] and simulates the dynamics of a ''society of living individuals'' in the presence of noise.

II. THE MODEL AND THE MONTE CARLO SIMULATION METHOD

The model is a probabilistic cellular automaton (CA) (totalistic CA) defined on a square lattice. Each site of the lattice σ_{ij} can take only two values $\sigma_{ij}=\{0,1\}$ and interacts with its eight nearest neighbors. Using the notation of the Conway's game of life [18] (for details see [15]), we will refer to a site in the state $\sigma_{ij}=1$ ($\sigma_{ij}=0$) as a ''living site'' (''dead site''), respectively. The system evolves in time according to the following rules: (i) a living site whose neighborhood is dead (empty) or has one living site, will die in the next time step, (ii) a living site whose neighborhood has more than three living sites, will die in the next time step, (iii) a living site whose neighborhood has two or three living sites, will survive with a probability p_s in the next time step, (iv) a dead site whose neighborhood is dead (empty) or has one living site, will remain in this state in the next time step, (v) a dead site whose neighborhood has more than three living sites, will remain in this state in the next time step, (vi) a

*Present address: Department of Physics, Bar-Ilan University, Ramat-Gan 52900, Israel.

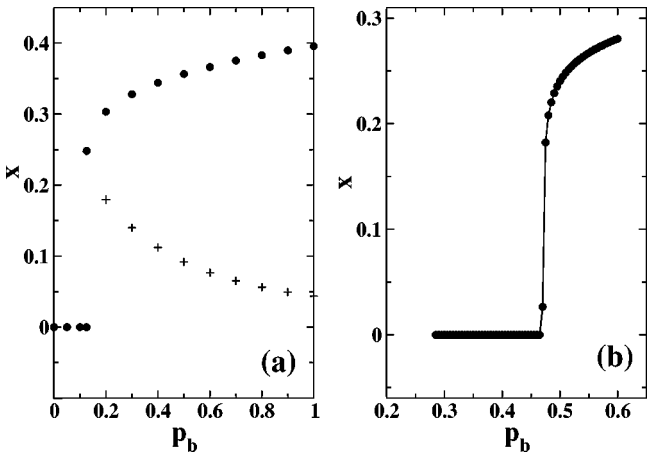

FIG. 1. Plots of the density of living sites x [in arbitrary units (AU)] versus p_b, keeping $p_s=0.10$. (a) Results obtained using the MF approximation. Full dots (plus signs) indicate stable (unstable) fixed points of Eq. (1). (b) Stationary simulation results obtained for a lattice of size $L=400$.

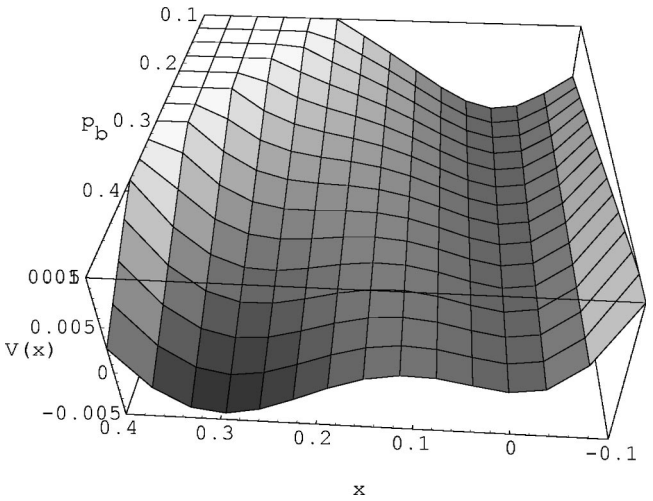

FIG. 2. 3D plot of the potential $V(x)$ (AU) versus x (AU) and p_b for $p_s=0.10$ fixed, corresponding to the SGL model. Darkest areas correspond to the potential minima.

dead site whose neighborhood has exactly two living sites, will become a living site with a probability p_b in the next time step, (vi) A dead site whose neighborhood has exactly three living sites, will always become a living site in the next time step.

As it is common in CA models, all sites are updated simultaneously. The parameters of the model have been selected in such a way that, for $p_s=1$ and $p_b=0$, the deterministic Conway's game of life is recovered. Initializing the system with a random distribution of living sites, the SGL evolves until reaching a stationary state. Simulation results show that the phase diagram of the system (p_s versus p_b) consists of two phases, namely, extinction (devoid of living sites) and a living phase, separated by a first-order critical curve [15].

III. MEAN-FIELD APPROACH

In order to obtain a qualitative description of the model, a mean-field (MF) analysis has been performed. This analysis, often called single site MF analysis, completely neglects correlations among sites. The method consists in writing down a equation for the time evolution of the density of living sites. Then, only local processes that increase or decrease the density, according to the evolution rules, are considered. The result is the following nonlinear first-order differential equation

$$\frac{dx}{dt}=x[-x^8-8x^7y-28x^6y^2-56x^5y^3-70x^4y^4-56(1-p_s)x^3y^5+28(1+p_s)x^2y^6+(28p_b-8)xy^7-y^8], \tag{1}$$

where x is the density of living sites and $y=1-x$. The fixed points of Eq. (1) satisfy $dx/dt=f(x)=0$, and the stable ones correspond to the stationary states of the lattice model. Figure 1(a) shows a plot of x versus p_b, for $p_s=0.10$, obtained by numerically solving $f(x)=0$. Stable (unstable) solutions of $f(x)=0$ are indicated with full dots (plus signs), respectively. It is clear from Eq. (1) that $x=0$ is always a solution of $f(x)=0$, which is stable for all p_s and p_b values. The solution $x=0$ has only been indicated in Fig. 1(a) for the values of p_b where this is the only fixed point of the system. This solution corresponds to the single absorbing state devoid of living sites of the lattice model. In addition, for larger values of p_b, there are two different branches of stationary solutions that coalesce at the MF critical point that is a saddle-node bifurcation. Figure 1(a) resembles the behavior of the density x obtained by means of simulations. In fact, Fig. 1(b) shows a jump in the density x around the coexistence point. However, since the MF approach neglects fluctuations, the value of the critical point given by this approach is an underestimate.

An alternative way to study the system is based on the idea of a potential function $V(x)$, defined through the following relation:

$$\frac{dx}{dt}=f(x)=-\frac{dV(x)}{dx}. \tag{2}$$

According to this definition, the stable (unstable) fixed points correspond to the minima (maxima) of $V(x)$, respectively. It is easy to show that

$$\frac{dV(x)}{dt}=-\left(\frac{dV(x)}{dx}\right)^2, \tag{3}$$

which indicates that the system always evolves towards the potential valleys. Figure 2 shows a 3D plot of the potential $V(x)$ versus x and p_b, keeping $p_s=0.10$ constant. Darkest regions on the surface indicate the minima of $V(x)$. The valley observed at $x=0$ corresponds to the stationary absorbing state of the lattice model. Figure 3 shows sections of the potential surface $V(x)$ for four different values of p_b. For values of p_b large enough [see Figs. 3(a) and 3(b)], a mini-

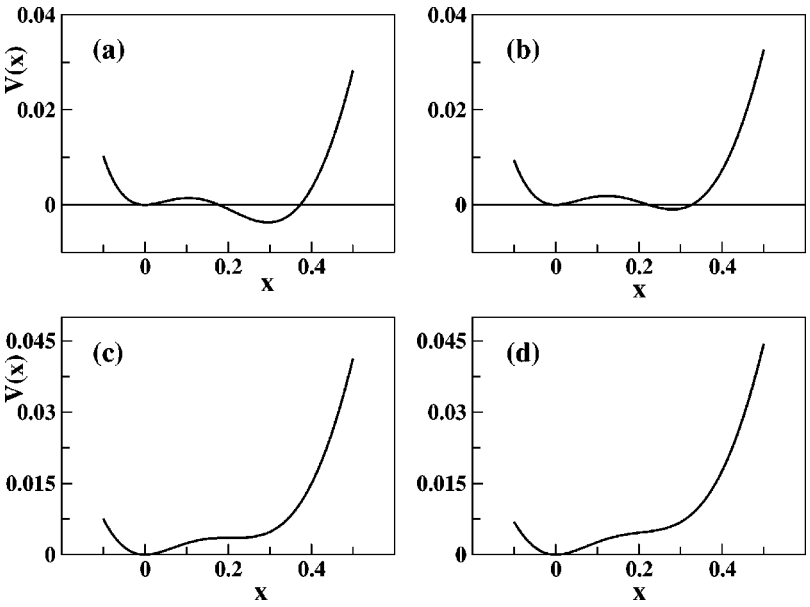

FIG. 3. Sections of the potential $V(x)$ (AU) shown in Fig. 2 corresponding to different values of the parameter p_b, (a) $p_b=0.45$, (b) $p_b=0.35$, (c) $p_b^c=0.3131$, and (d) $p_b=0.20$.

mum at a higher density $x=x_h$ and a maximum are observed. This minimum corresponds to a stationary state that belongs to the living phase. For p_s fixed, the relative position of x_h with respect to $x=0$ depends on the value of p_b. As mentioned above, the minimum at a higher density vanishes when decreasing p_b. The pair of values (p_s^c, p_b^c) where this minimum just disappears is the MF critical point. Further decreasing p_s leads to potential functions displaying only one minimum at $x=0$ [see Fig. 3(d)]. Figures 3(c) and 3(d) clearly show that the minimum at a higher density disappears at a value x_c well above $x=0$. In other words, a sharp jump is observed in the order parameter of the system (x) when decreasing the value of the parameter p_b. Then, the MF approach predicts a first-order IPT that is in full agreement with simulation results [15]. It should be noted that the order of the IPT predicted by the MF approximation rarely agree with simulation results in low dimensions. In fact, while simulations often show second-order irreversible critical behavior in low dimensions, MF approaches may predict a first-order behavior. In some cases, by including processes such as a high diffusion in a lattice model, the second-order critical behavior may turn into a first-order behavior, as predicted by the MF approach [19].

It should be noticed that as the system always evolves to the potential valleys the stationary state will depend upon the initial density, i.e., $x_0=x(t=0)$ [see Figs. 3(a) and 3(b)]. In simulations, the stationary state depends not only on the initial density but also on the spatial distribution of living sites.

The MF critical points can be calculated by solving the following system of equations:

$$\frac{dV(x)}{dx}=0 \wedge \frac{d^2V(x)}{dx^2}=0. \tag{4}$$

Figures 4(a) and 4(b) show the phase diagram obtained by means of the MF approximation and simulations, respectively. Since fluctuations are not considered in the MF treatment, the MF living phase is larger than the one obtained by simulations.

IV. RESULTS AND DISCUSSION

We have studied in detail two main aspects of the SGL model, namely, the memory effects and the dynamical critical behavior.

A. Memory effects

Hysteresis effects are studied by means of the spontaneous creation method (SCM) [20]. In the SCM, a very small creation rate of living sites (active sites) κ is introduced for sites whose neighborhood is devoid of living sites. First, a pair of values (p_s, p_b) within the living phase is chosen and the system evolves until reaching a stationary state. Then, one of the parameters of the models is kept constant (p_s in this case) and the other one (p_b) is varied stepwise after time

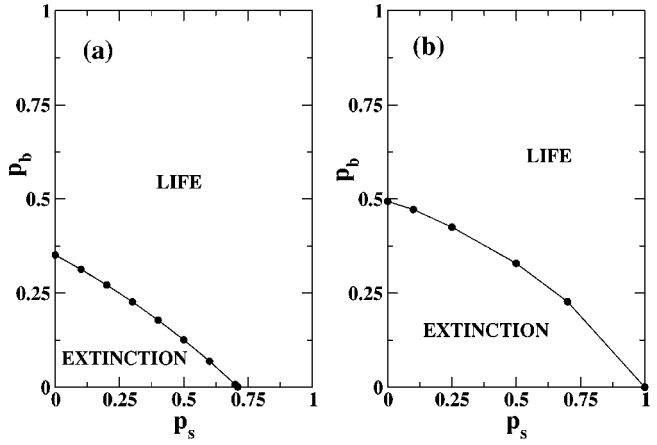

FIG. 4. Phase diagram of the SGL model. (a) Results obtained by solving Eqs. (4). (b) Simulation results taken from Ref. [15].

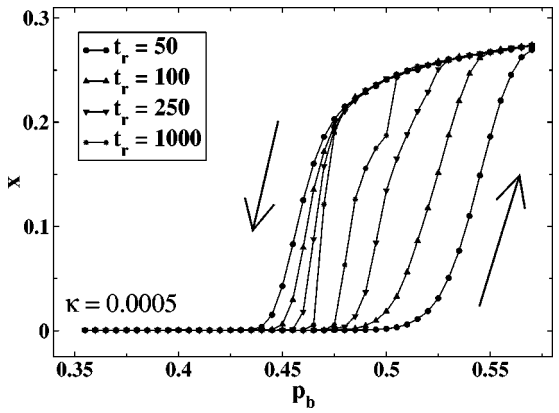

FIG. 5. Hysteresis loops of the density x (AU) obtained by means of the SCM using a lattice of size $L=200$ for different relaxation times t_r (in lattice updates) and keeping $p_s=0.10$ and $\kappa=0.0005$ fixed. Loops are generated counterclockwise (see arrows).

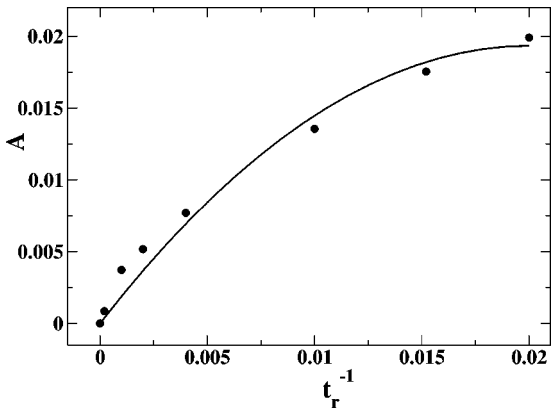

FIG. 6. Area A (AU) of the hysteresis loops shown in Fig. 5 versus t_r^{-1} (in lattice updates)$^{-1}$. The full curve corresponds to the best second-order polynomial fitting $A=s(1.93-47.98s)$. More details in the text.

intervals of t_r updates so as to complete a cycle. After t_r updates, a value of the density x is recorded and averages are taken over different loops. It should be noticed that for second-order IPT's, a spontaneous creation rate of active sites will destroy the phase transition. However, for first-order IPT's a small spontaneous creation rate will not change the nature of the transition but turns the absorbing state into a fluctuating state of average density κ, allowing for the study of hysteresis effects. The presence of hysteresis effects will be a signature of a first-order IPT. Figure 5 shows a plot of x versus p_b for different relaxation times t_r obtained by means of the SCM. The hysteresis effects evident in Fig. 5 can be explained on the basis of the MF approach (see Fig. 3). In fact, a small creation rate does not alter the MF scenario except for the positions of the potential minima that are slightly shifted. Starting the loop at a living stationary state [absolute minimum in Fig. 3(a)], the value of the parameter p_b is decreased stepwise after a relaxation time t_r. Then, a characteristic evolution of the potential function $V(x)$ follows the sequence Figs. 3(b)–3(d). It should be noted that the MF approach neglects density fluctuations. However, density fluctuations can be thought as small oscillations around the value of the potential minimum. These fluctuations allow for the transition between minima, i.e., there is a finite probability to overcome the potential barrier. Figure 5 shows that for different values of t_r, the decreasing branches are closer to each other than the corresponding growing branches. This asymmetry observed in the hysteresis loops is due to the asymmetry of the potential function. In fact, starting at a living stationary state [see Fig. 3(a)], the potential barrier decreases when decreasing the value of the parameter p_b and eventually vanishes [see Fig. 3(d)]. However, starting at a low density stationary state [see Fig. 3(d)], the system always has to overcome a potential barrier in order to jump to the higher density state, even though this state is the absolute minimum of the potential [see Fig. 3(a)]. The waiting time t_w, which is the average time needed to overcome the potential barrier, grows with the height of the barrier. For $t_r \sim t_w$, a critical drop of the stable phase develops that eventually spreads over the whole system. That is why the longer the relaxation time the inner the loop. This feature is quantified in Fig. 6 where a plot of the area A of the loops versus t_r^{-1} is shown. Figure 6 shows that the loop area is not a linear function of t_r^{-1} but can be approximated using the following second-order polynomial:

$$A=s(K_1-K_2 s), \tag{5}$$

where $s\equiv t_r^{-1}$, $K_1=1.93$, and $K_2=47.98$. It should be noted that for infinite relaxation time ($s\to 0$), memory effects have to vanish. This condition is satisfied by Eq. (5).

B. Epidemics analysis

The dynamical critical behavior of second-order IPT is usually studied by means of the epidemic analysis (EA) [4,9] where the time evolution of relevant quantities display a power-law behavior at the critical point. EA has been also applied to first-order IPT [14,15]. These results claim the existence of scale invariance in the dynamical critical behavior of first-order IPT. We will show that for this system the asymptotic time behavior is exponentially growing or decaying depending on the value of the parameter.

EA simulations are normally initialized placing a small colony of active sites into an otherwise absorbing state. This choice allows the system to quickly achieve the asymptotic time regime. It is shown, however, that this choice is misleading for the present model and hinder the real asymptotic regime that is by no means universal.

We studied the time evolution of the average number of living sites $N(t)$, initializing the simulation with colonies of different sizes. For cellular automata with parallel updating, time t is given in number of updates. We have developed an optimized algorithm that allows us to monitor the time evolution of the system up to very long times and free from finite-size effects. The algorithm is initialized placing some activity around the center of the sample within a region of size $l\times l$ ($l\ll L$), i.e., at $t=0$ only a sublattice of size $(l+1)\times(l+1)$ needs to be visited. Since activity may only arise in the neighborhood of active sites (see evolution rules), we first find the coordinates of the outermost sites

with respect to the center along each direction of the system, namely, l_x^{min}, l_x^{max}, l_y^{min}, and l_y^{max}, and in the next time step update a system of size $(l_x^{max}-l_x^{min}+2)$ x $(l_y^{max}-l_y^{min}+2)$. It should be noticed that this improved method is dynamic since l_x^{min}, l_x^{max}, l_y^{min}, and l_y^{max} are fluctuating quantities. Averages are taken over 10^5-10^8 different samples.

Figure 7(a) shows a plot of $N(t)$ versus t obtained by using an initial colony of five living sites (called glider in the Conway's game of life zoo) and for different values of p_b keeping $p_s=0.10$ fixed. We clearly observe that the asymptotic regime is reached after $t>10^4$ updates and it is possible to identify subcritical and supercritical curves. The apparent critical behavior observed at $p_s=0.471\,88$ is because the asymptotic regime has not yet been achieved for this value of the parameter. Eventually, this curve will exponentially grow or decay. The point $(p_s=0.10, p_b=0.471\,88)$ is actually a good estimate of the upper spinodal point [19]. In addition, $N(t)$ displays a short-time regime $(t<10^2)$ and an intermediate-time regime $(10^2<t<10^4)$, the last resembling a plateau behavior. Figure 7(b) is similar to Fig. 7(a) but a log-lineal scale is used. It is clearly observed that the asymptotic regime is exponential. It should be noted that $N(t)$ is remarkably sensitive to tiny changes in the values of the parameters that is characteristic of first-order IPT's.

Figure 7(c) is similar to Fig. 7(a) except for the use of a bigger colony to initialize the EA. The following three main differences are observed: (i) the short-time behavior present in Fig. 7(a) is absent; (ii) the intermediate-time regime dominates from the very beginning, and (iii) the asymptotic regime is achieved sooner $(t\approx 10^3)$. These features can be understood on the basis of the potential $V(x)$. Let us focus on both Fig. 3(c), which shows the potential function $V(x)$ at criticality, and a potential function slightly above criticality displaying two minima (not shown in Fig. 3). For low initial densities, Eq. (3) indicates that x will flow to $x=0$, the density of the stationary absorbing state. This explains why $N(t)$ displays a decreasing short-time behavior in Fig. 7(a). Decreasing short-time behavior appears to be a universal feature observed, to our best knowledge, in first-order IPT to a unique absorbing state [7,15,16,19]. As mentioned above, density fluctuations can be considered as oscillations around the potential minima. In some few cases, a density fluctuation may overcome the potential barrier placing the system in a region where $V(x)\approx$const. Consequently, the system can remain for a long time in a region free from driving forces until another large fluctuation drives it either towards $x=0$ or to the living stationary state. This explains the plateau observed in the intermediate-time regime and the asymptotic regime as well. Another way of corroborating the above explanation is provided by Fig. 7(c). In this case, the initial density is in a region where $V(x)\approx$const from the beginning. That is why the short-time behavior is absent and only the plateau and the asymptotic behavior remain.

The intermediate-time behavior can also be explained by means of Eq. (1). Figure 8 shows a plot of dx/dt versus x for a value of p_b slightly below the critical point p_b^c. Within the neighborhood of the critical point $f(x)$ can be approximated

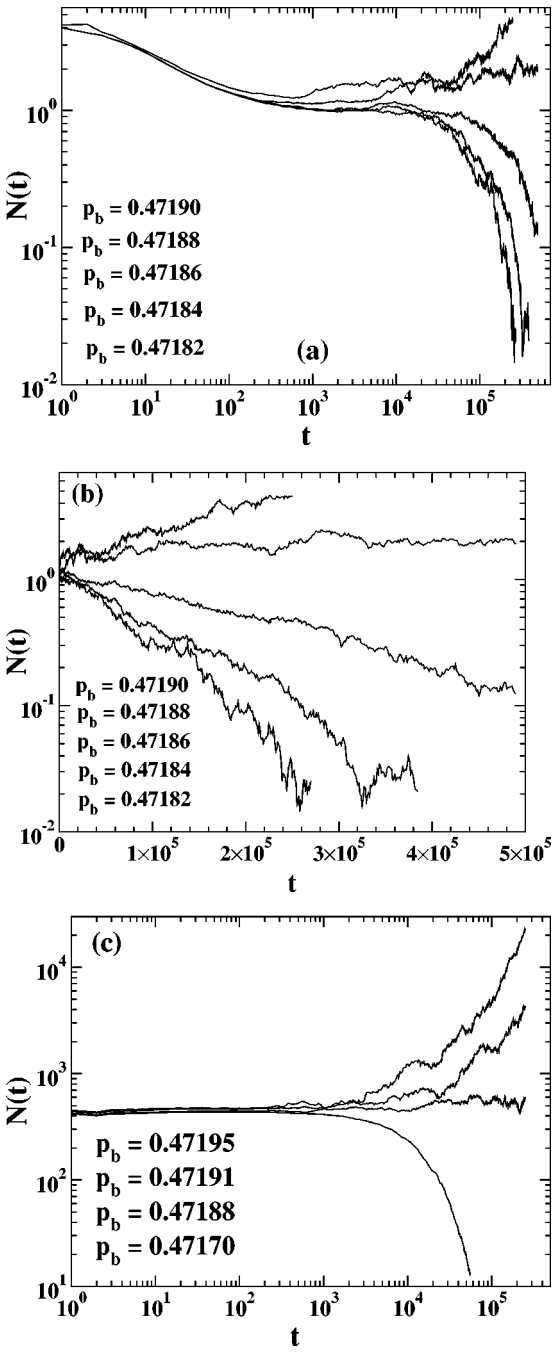

FIG. 7. Log-log plots of the average number of living sites $N(t)$ (AU) versus t (in lattice updates) for different values of the parameter p_b, keeping $p_s=0.10$ fixed. From top to bottom, the values of p_b indicated in the figures correspond to each curve, respectively. (a) The EA was initialized using a small colony of living sites. (b) Idem (a) but using a log-lineal scale. The exponential decay and growth of $N(t)$ are clearly observed. (c) The EA was initialized by randomly filling a 50×50 sublattice located in the middle of the system with probability $p=0.15$.

by a Taylor expansion up to second order

$$\frac{dx}{dt}=-r-a(x-x_0)^2, \tag{6}$$

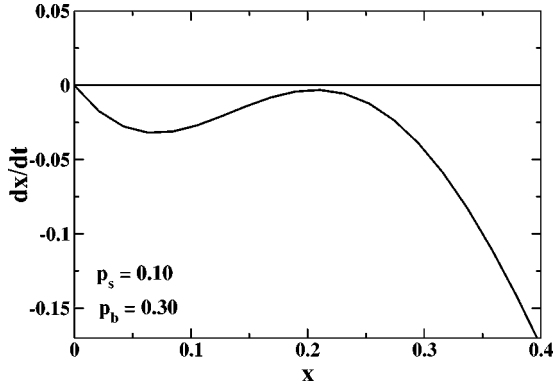

FIG. 8. Plot of dx/dt (AU) versus x (AU) obtained using Eq. (1). In this case, the stationary state of the system is the absorbing state. Note, however, that the values of the parameters are close to the critical point.

where $(x_0,-r)$ are the coordinates of the vertex and a is the curvature of the parabola. Notice that r and a are positive numbers. For $p_b<p_b^c$, the system will flow towards the only stable fixed point at $x=0$. Now, we estimate the time τ needed to reach the fixed point. It is clear from Eq. (6) that the main contribution to this time comes from the immediate vicinity of the maximum, since the time spent there dominates all other time scales in the system. The result is given by the following equation:

$$\tau=-\int_{x_0+\Delta}^{x_0-\Delta}\frac{dx}{r+a(x-x_0)^2}=2\frac{1}{\sqrt{ar}}\tan^{-1}(\sqrt{a/r}\Delta), \quad (7)$$

where $0<\Delta\ll 1$ is a constant. Then, we conclude from Eq. (7) that when p_b gets closer to the critical point, i.e., when the parameter r approaches zero, the time needed by the system to reach the fixed point becomes longer. So, the dynamics of the system becomes very slow in the neighborhood of a ''ghost'' fixed point. This finding is in complete agreement with simulation results. In fact, Fig. 7(a) shows that the plateau behavior last longer for p_b nearer to the upper spinodal point, i.e., the time spent to finally reach the fixed point increases. The position of the coexistence point is very difficult to determine for a discontinuous IPT. Constant coverage simulations [16,21] have proven to give very good estimates of the position of this point that is very close to the coexistence point for weak first-order IPT's. Finally, it should be remarked that the intermediate regime is characteristic of this model and it is not a universal feature of first-order IPT [16].

Figure 9 shows two plots of $N(t)$ versus t for values of p_b in the critical neighborhood obtained by using an initial colony of five living sites. Figure 9(b) shows that the short-time behavior of the system can be easily confused with a power-law behavior [14,15].

V. CONCLUSIONS AND FINAL REMARKS

In summary, the first-order critical behavior of the SGL model has been studied using extensive computer simulations and a MF approximation. The results obtained by means of the single site mean-field analysis are in remarkably good qualitative agreement with simulation results. The mean-field theory predicts the first-order IPT observed in the lattice model and qualitatively explains both hysteresis effects and the dynamical critical behavior observed in the epidemic analysis. The intermediate plateau behavior observed in epidemic simulations is the result of the critical slowing down predicted by the MF approach. It should be remarked that results based on inadequately short-time simulations are not sufficient to ensure the existence of a power-law behavior. In fact, the asymptotic time regime of this system behaves exponentially. Then, the occurrence of power laws in the dynamical critical behavior of first-order IPT's can be safely ruled out. This last finding conciliates the behavior of first-order IPT's with their counterpart in equilibrium systems where it is well established that the existence of short range correlations inhibits the observation of scale invariance.

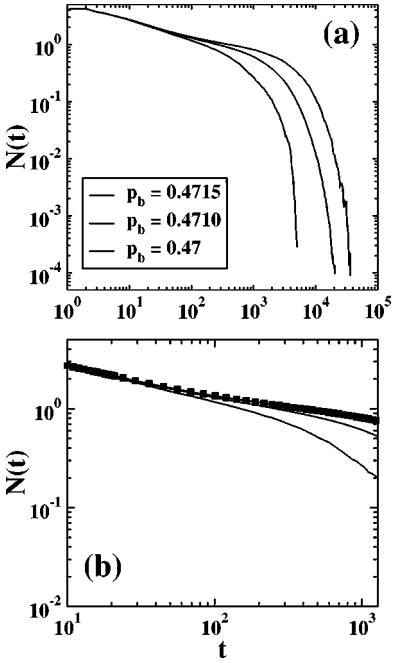

FIG. 9. Log-log plots of the average number of living sites $N(t)$ (AU) versus t (in lattice updates) for different values of the parameter p_b, keeping $p_s=0.10$ fixed. From top to bottom, the values of p_b indicated in the figure correspond to each curve, respectively. (a) The complete evolution of $N(t)$, (b) A region is shown where the dynamical behavior of the curve indicated with full squares resembles a power law.

ACKNOWLEDGMENTS

This work was supported by CONICET, UNLP, ANPCyT, Fundación Antorchas (Argentina), and Volkswagen Foundation (Germany). I would like to acknowledge illuminating discussions with Ezequiel Albano, Shlomo Havlin, and Alejandro Rozenfeld.

[1] See a set of papers published in Science **284**, 79 (1999).
[2] J. Marro and R. Dickman, in *Non-equilibrium Phase Transitions in Lattice Models* (Cambridge University Press, Cambridge, 1999).
[3] E.V. Albano, Heterog. Chem. Rev. **3**, 389 (1996).
[4] P. Grassberger and A. de la Torre, Ann. Phys. (N.Y.) **122**, 373 (1979); P. Grassberger, J. Phys. A **22**, 3673 (1989).
[5] H.K. Janssen, Z. Phys. B: Condens. Matter **42**, 151 (1981); P. Grassberger, *ibid.* **47**, 365 (1982).
[6] M. Moshe, Phys. Rep. **37**, 255 (1978).
[7] R. Ziff, E. Gulari, and Y. Barshad, Phys. Rev. Lett. **56**, 2553 (1986).
[8] I. Jensen, H. Fogedby, and R. Dickman, Phys. Rev. A **41**, 3411 (1990).
[9] I. Jensen, Phys. Rev. Lett. **70**, 1465 (1993).
[10] I. Jensen and R. Dickman, Phys. Rev. E **48**, 1710 (1993); I. Jensen, J. Phys. A **27**, L61 (1994); D.H. Linares, E.V. Albano, and R.A. Monetti, *ibid.* **32**, 8023 (1999).
[11] A. Vespignani, R. Dickman, M.A. Muñoz, and S. Zapperi, Phys. Rev. Lett. **81**, 5676 (1998); Phys. Rev. E **62**, 4564 (2000); M. Rossi, R. Pastor-Satorras, and A. Vespignani, Phys. Rev. Lett. **85**, 1803 (2000); R. Dickman, M. Alava, M.A. Muñoz, J. Peltola, A. Vespignani, and S. Zapperi, e-print cond-mat/0101381.
[12] J.L. Cardy and U.C. Täuber, J. Stat. Phys. **90**, 1 (1998); R.A. Monetti, Phys. Rev. E **58**, 144 (1998).
[13] M. Ehsasi *et al.*, J. Chem. Phys. **91**, 4949 (1989); R. Imbihl, Prog. Surf. Sci. **44**, 185 (1993); G. Ertl, Adv. Catal. **37**, 213 (1990).
[14] J.W. Evans and M.S. Miesch, Phys. Rev. Lett. **66**, 833 (1991); Surf. Sci. **245**, 401 (1991); J.W. Evans and T.R. Ray, Phys. Rev. E **50**, 4302 (1994).
[15] R.A. Monetti and E.V. Albano, Phys. Rev. E **52**, 5825 (1995); J. Theor. Biol. **187**, 183 (1997).
[16] R.A. Monetti and E.V. Albano, J. Phys. A **34**, 1106 (2001).
[17] F. Gulminelli and Ph. Chomaz, Phys. Rev. Lett. **82**, 1402 (1999).
[18] E. R. Berlekamp, J. H. Conway, and R. K. Guy, *Winning Ways for your Mathemetical Plays* (Academic, New York, 1982), Vol. 2.
[19] R. Dickman and T. Tomé, Phys. Rev. A **44**, 4833 (1991).
[20] R. Bidaux, N. Boccara, and H. Chaté, Phys. Rev. A **39**, 3094 (1989).
[21] R. Ziff and B.J. Brosilow, Phys. Rev. A **46**, 4630 (1992).